
STUDY OF FLOW AND HEAT TRANSFER BEHAVIOR OF
THREE DIMENSIONAL MHD NANOFUID FLOW
CONSIDERING THERMAL INTERFACIAL RESISTANCE
AND MICRO MIXING IN SUSPENSIONS

Content of this chapter is published in:

- Chinese Journal of Physics (Elsevier). 55 (2017) 2254 – 2272.
- Mathematics Today, 34 (A) (2018) 7-24, ISSN 0976-3228

STUDY OF FLOW AND HEAT TRANSFER BEHAVIOR OF THREE DIMENSIONAL MHD NANOFUID FLOW CONSIDERING THERMAL INTERFACIAL RESISTANCE AND MICRO MIXING IN SUSPENSIONS

Many of the real world problems require three dimensional mathematical modelling, so the problems discussed in previous chapters need to be extended to three dimension. In this chapter, effect of magnetic field on three dimensional nanofluid flow between two horizontal parallel plates through porous medium is scrutinized. System under consideration is rotating. Effects of thermal interfacial resistance, nanoparticle volume fraction, Brownian motion, nanoparticle size, types of nanoparticle and base fluid on thermal conductivity are considered. Also, micro mixing in suspensions is taken into account while calculating viscosity.

7.1 Introduction

From an energy saving perception, enhancement of heat transfer performance in systems is vital subject. Low thermal conductivity of orthodox fluids such as water and oils is a key limitation in improving the performance of systems. Solids usually have a higher thermal conductivity than liquids. For example, aluminum (Al) has a thermal conductivity 350 times greater than water and 1500 times greater than engine oil. This limitation of the conventional fluids can be overcome by replacing them with nanofluids. Enhancement of heat transfer is vital in Industrial and engineering processes. High thermal conductivity of nanofluids is a boon in this direction, thus many researchers are working intensively considering heat transfer properties of nanofluids.

Effect of magnetic field on electrically conducting fluids has many applications in almost all branches of science and engineering such as generators, coolant in huge nuclear power plants, plasma and bearings. Magnetohydrodynamics effect on convective flow of nanofluid was studied by Hayat et al. [23].

Oil extraction, Pollution of Ground water, filtering media, geothermal energy recovery and thermal energy storage are some problems involving heat transfer in porous media. Sheikholeslami and Shehzad [97] studied MHD nanofluid convective flow in a porous enclosure. Kataria and Mittal [30 - 31] analyzed velocity, mass and temperature of nanofluid flow in a porous medium.

In real world problems, thermal radiation is evident which is reflected in study of various researchers. Kataria and Mittal [29] discussed optically thick nanofluid flow past an oscillating vertical plate in presence of radiation. Sheikholeslami et al. [64] examined heat transfer characteristics in nanofluid flow between two horizontal parallel plates in a rotating system.

7.2 Novelty of the Problem

The aim of this study is to analyze heat transfer in nanofluid flow in presence of magnetic field and thermal radiation between horizontal parallel plates in a rotating system. Effects of many vital phenomenon like thermal interfacial resistance, nanoparticle volume fraction, Brownian motion and nanoparticle's size on thermal conductivity are often neglected.

Novelty of the present work is the inclusion of above phenomenon along with micro mixing in suspensions. The simplified system of ordinary differential equations are solved using the HAM. The effects of the pertinent parameters are discussed.

7.3 Mathematical Formulation of the Problem

Fluid under consideration is Al_2O_3 – water nanofluid. Flow is assumed to be between two horizontal parallel plates L units apart through a porous medium. A coordinate system (x, y, z) is chosen such that origin is positioned at the lower plate and axis as shown in Figure 7.1. The lower plate is subject to stretching by two opposite forces in opposite directions. The plates along with the fluid rotate about y axis with angular velocity Ω . A uniform magnetic flux with density B is applied along y -axis.

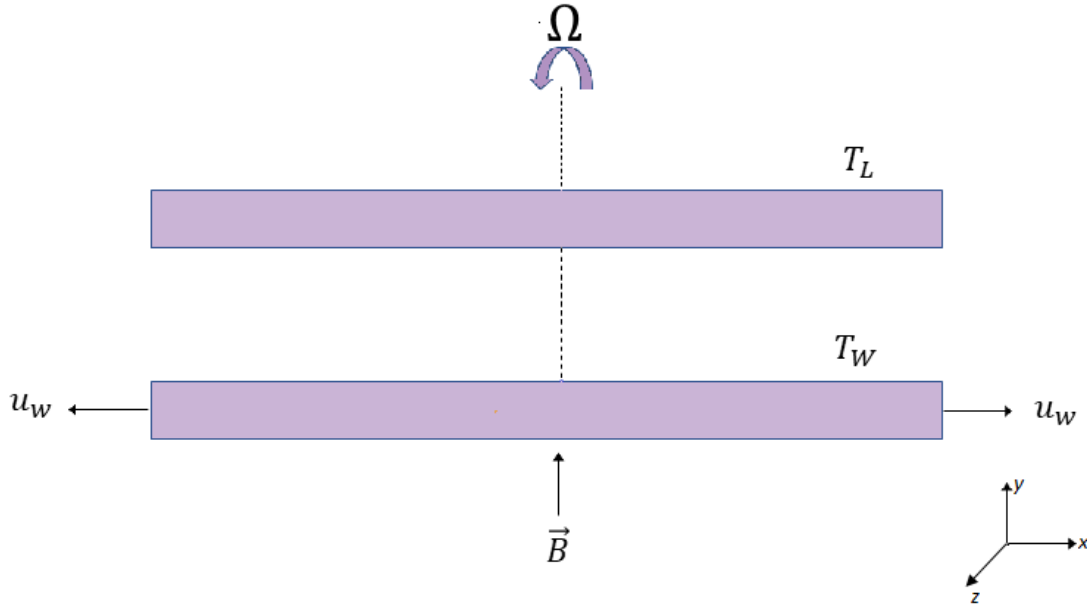


Figure 7.1: Physical Sketch of the Problem

Under these assumptions, governing equations are:

$$\frac{\partial u}{\partial x} + \frac{\partial v}{\partial y} + \frac{\partial w}{\partial z} = 0, \quad (7.1)$$

$$\rho_{nf} \left(u \frac{\partial u}{\partial x} + v \frac{\partial u}{\partial y} + 2\Omega w \right) = \mu_{nf} \left(\frac{\partial^2 u}{\partial x^2} + \frac{\partial^2 u}{\partial y^2} \right) - \sigma_{nf} B^2 u - \frac{\mu_{nf} \phi}{k_1} u, \quad (7.2)$$

$$\rho_{nf} \left(u \frac{\partial v}{\partial y} \right) = \mu_{nf} \left(\frac{\partial^2 v}{\partial x^2} + \frac{\partial^2 v}{\partial y^2} \right), \quad (7.3)$$

$$\rho_{nf} \left(u \frac{\partial w}{\partial x} + v \frac{\partial w}{\partial y} - 2\Omega w \right) \frac{\partial w}{\partial z} = \mu_{nf} \left(\frac{\partial^2 w}{\partial x^2} + \frac{\partial^2 w}{\partial y^2} \right) - \sigma_{nf} B^2 w - \frac{\mu_{nf} \phi}{k_1} w, \quad (7.4)$$

$$\begin{aligned} (\rho c_p)_{nf} \left(u \frac{\partial T}{\partial x} + v \frac{\partial T}{\partial y} + w \frac{\partial T}{\partial z} \right) &= k_{nf} \left(\frac{\partial^2 T}{\partial x^2} + \frac{\partial^2 T}{\partial y^2} + \frac{\partial^2 T}{\partial z^2} \right) + \mu_{nf} \left(2 \left[\left(\frac{\partial u}{\partial x} \right)^2 + \left(\frac{\partial v}{\partial y} \right)^2 + \left(\frac{\partial w}{\partial z} \right)^2 \right] + \right. \\ &\quad \left. \left(\frac{\partial v}{\partial x} \right)^2 + \left(\frac{\partial v}{\partial z} \right)^2 + \left(\frac{\partial w}{\partial x} + \frac{\partial u}{\partial z} \right)^2 \right) - \frac{\partial q_r}{\partial y}, \end{aligned} \quad (7.5)$$

where

$$\rho_{nf} = (1 - \phi)\rho_f + \phi\rho_s, \quad (7.6)$$

$$\sigma_{nf} = \sigma_f \left[1 + \frac{3(\sigma-1)\phi}{(\sigma+2) - (\sigma-1)\phi} \right], \quad \sigma = \frac{\sigma_s}{\sigma_f}, \quad (7.7)$$

$$(\rho c_p)_{nf} = (1 - \phi)(\rho c_p)_f + \phi(\rho c_p)_s. \quad (7.8)$$

Effects of thermal interfacial resistance, nanoparticle volume fraction, Brownian motion and nanoparticle's size on thermal conductivity are considered. Also, micro mixing in suspensions is taken into account while calculating viscosity.

$$k_{eff} = k_{static} + k_{Brownian} = k_f \left[1 - 3 \frac{\phi(k_f - k_{s,R})}{2k_f + k_{s,R} + \phi(k_f - k_{s,R})} \right] + 5 \times 10^4 \phi \rho_f c_{pf} \sqrt{\frac{\kappa_b T}{\rho_s d_s}} F(T, \phi, d_s), \quad (7.9)$$

$$k_{s,R} = \frac{k_s d_s}{R_f k_s + d_s}, \quad (7.10)$$

$$F(T, \phi, d_s) = (A_1 + A_2 \ln(d_s) + A_3 \ln(\phi) + A_4 \ln(\phi) \ln(d_s) + A_5 \ln(d_s^2)) \ln(T) + (A_6 + A_7 \ln(d_s) + A_8 \ln(\phi) + A_9 \ln(\phi) \ln(d_s) + A_{10} \ln(d_s^2)), \quad (7.11)$$

with

$R_f = 4 * 10^{-8} Km^2/W$ is thermal interfacial resistance,

$$A_1 = 52.813488759, \quad A_2 = 6.115637295, \quad A_3 = 0.6955745084, \quad A_4 = .0417455552786,$$

$$A_5 = 0.176919300241, \quad A_6 = -298.19819084, \quad A_7 = -34.532716906, \quad A_8 = -3.9225289283,$$

$$A_9 = -0.2354329626, \quad A_{10} = -0.999063481. \quad (7.12)$$

(Here it must be noted that these values are not general and vary with nanofluids.)

Considering effects of micro mixing in suspensions on viscosity,

$$\mu_{nf} = \mu_{static} + \mu_{Brownian} = \frac{\mu_f}{(1-\phi)^{2.5}} + \frac{k_{Brownian} * \mu_f}{k_f * Pr_f}. \quad (7.13)$$

Considering temperature difference within the flow to be sufficiently small, using Taylor's series and neglecting higher terms, q_r [61] becomes

$$q_r = -\frac{4\sigma^*}{3k^*} \frac{\partial T^4}{\partial y} = -\frac{4\sigma^*}{3k^*} \frac{\partial(4T_0^3 T - 3T_0^4)}{\partial y}. \quad (7.14)$$

The thermo-physical properties of water and nanoparticles are as in Table 1.1.

Boundary conditions are

$$u = ax; v = 0; w = 0; T = T_w \text{ at } y = 0, \quad (7.15)$$

$$u = 0; v = 0; w = 0; T = T_L \text{ at } y = L. \quad (7.16)$$

Introducing non dimensional variables

$$\eta = \frac{y}{L}, u = axf'(\eta), v = -ahf(\eta), w = axg(\eta), \theta(\eta) = \frac{T-T_L}{T_w-T_L}. \quad (7.17)$$

Therefore, the governing momentum and energy equations for this problem are given in dimensionless form by:

$$a_1 f^{iv} - Re(f'f'' - ff''') - 2Krf' - \left(a_3 M^2 + \frac{a_1}{k}\right) f'' = 0, \quad (7.18)$$

$$a_1 g'' - Re(f'g - fg') + 2Krf' - \left(a_3 M^2 + \frac{a_1}{k}\right) g = 0, \quad (7.19)$$

$$\theta'' + Pr(Rea_2 f\theta' + Eca_4(4f'^2 + g^2)) = 0, \quad (7.20)$$

where

$$Pr = \frac{\mu_f (c_p)_f}{k_f}, M^2 = \frac{\sigma_f B_0^2 L^2}{\rho_f \nu_f}, \frac{1}{\kappa} = \frac{\nu \varphi^2}{k_1 \nu_f}, Kr = \frac{\Omega L^2}{\nu_f}, Re = \frac{aL^2}{\nu_f}, Ec = \frac{(aL)^2}{(c_p)_f (\theta_0 - \theta_L)}, \quad (7.21)$$

$$b_0 = 1 - \phi, \quad (7.22)$$

$$b_1 = (b_0 + \phi \frac{\rho_s}{\rho_f}), \quad (7.23)$$

$$b_2 = \frac{1}{b_0^{2.5}}, \quad (7.24)$$

$$b_3 = (b_0 + \phi \frac{(\rho c_p)_s}{(\rho c_p)_f}), \quad (7.25)$$

$$b_4 = \frac{k_{nf}}{k_f}, \quad (7.26)$$

$$b_5 = \frac{\sigma_{nf}}{\sigma_f}, \quad (7.27)$$

$$a_1 = \frac{1}{b_0^{2.5} b_1}, \quad (7.28)$$

$$a_2 = \frac{b_3}{b_4 + Nr}, \quad (7.29)$$

$$a_3 = \frac{b_5}{b_1}, \quad (7.30)$$

$$a_4 = \frac{b_2}{b_4}, \quad (7.31)$$

$$Nr = \frac{16\sigma^* T_0^3}{3k^* k_f}; \quad (7.32)$$

subject to

$$f = 0, f' = 1, g = 0, \theta = 1 \text{ at } \eta = 0, \quad (7.33)$$

$$f = 0, f' = 0, g = 0, \theta = 0 \text{ at } \eta = 1. \quad (7.34)$$

7.4 Solution by Homotopy analysis Method

Equations (7.18) – (7.20) are coupled non-linear ordinary differential equations and exact solutions are not known. To solve these equations together with the boundary conditions (7.33) – (7.34), HAM [40] is applied.

Initial guess is given by:

$$f_0(\eta) = \frac{-2}{e^2 - 4e + 3} + \frac{e-1}{e-3}\eta + \frac{2-e}{e^2 - 4e + 3}e^\eta + \frac{e}{e^2 - 4e + 3}e^{-\eta}; \quad g_0(\eta) = 0; \quad \theta_0(\eta) = 1 - \eta; \quad (7.35)$$

with auxiliary linear operators:

$$L_f = \frac{\partial^4 f}{\partial \eta^4} - \frac{\partial^2 f}{\partial \eta^2}, \quad L_g = \frac{\partial^2 g}{\partial \eta^2} - \frac{\partial g}{\partial \eta}, \quad L_\theta = \frac{\partial^2 \theta}{\partial \eta^2}, \quad (7.36)$$

satisfying

$$L_f(C_1 + C_2 \eta + C_3 e^\eta + C_4 e^{-\eta}) = 0, \quad L_g(C_5 + C_6 e^\eta) = 0, \quad L_\theta(C_7 + C_8 \eta) = 0, \quad (7.37)$$

where c_1, c_2, \dots, c_8 are the arbitrary constants.

The zeroth order deformation problems are constructed as follows:

$$(1 - p)L_f[\hat{f}(\eta; p) - f_0(\eta)] = p\hbar_f N_f[\hat{f}(\eta; p), \hat{g}(\eta; p), \hat{\theta}(\eta; p)], \quad (7.38)$$

$$(1 - p)L_g[\hat{g}(\eta; p) - g_0(\eta)] = p\hbar_g N_g[\hat{f}(\eta; p), \hat{g}(\eta; p), \hat{\theta}(\eta; p)], \quad (7.39)$$

$$(1 - p)L_\theta[\hat{\theta}(\eta; p) - \theta_0(\eta)] = p\hbar_\theta N_\theta[\hat{f}(\eta; p), \hat{g}(\eta; p), \hat{\theta}(\eta; p)], \quad (7.40)$$

subject to the boundary conditions:

$$\hat{f}(0; p) = 0, \quad \hat{f}'(0; p) = 1; \quad (7.41)$$

$$\hat{f}(1; p) = 0, \quad \hat{f}'(1; p) = 0; \quad (7.42)$$

$$\hat{g}(0; p) = 0, \quad \hat{g}(1; p) = 0; \quad (7.43)$$

$$\hat{\theta}(0; p) = 1, \quad \hat{\theta}(1; p) = 0. \quad (7.44)$$

The nonlinear operators are defined as

$$N_f[\hat{f}(\eta; p), \hat{g}(\eta; p), \hat{\theta}(\eta; p)] = a_1 \frac{\partial^4 \hat{f}}{\partial \eta^4} - Re \left(\frac{\partial \hat{f}}{\partial \eta} \frac{\partial^2 \hat{f}}{\partial \eta^2} - \hat{f} \frac{\partial^3 \hat{f}}{\partial \eta^3} \right) - 2Kr \frac{\partial \hat{g}}{\partial \eta} - \left(a_3 M^2 + \frac{a_1}{k} \right) \frac{\partial^2 \hat{f}}{\partial \eta^2}, \quad (7.45)$$

$$N_g[\hat{f}(\eta; p), \hat{g}(\eta; p), \hat{\theta}(\eta; p)] = a_1 \frac{\partial^2 \hat{g}}{\partial \eta^2} - Re \left(g \frac{\partial \hat{f}}{\partial \eta} - \hat{f} \frac{\partial g}{\partial \eta} \right) + 2Kr \frac{\partial \hat{f}}{\partial \eta} - \left(a_3 M^2 + \frac{a_1}{k} \right) g, \quad (7.46)$$

$$N_\theta[\hat{f}(\eta; p), \hat{g}(\eta; p), \hat{\theta}(\eta; p)] = \frac{\partial^2 \hat{\theta}}{\partial \eta^2} + Pr \left(Re a_2 \hat{f} \frac{\partial \hat{\theta}}{\partial \eta} + Eca_4 \left(4 \left(\frac{\partial \hat{f}}{\partial \eta} \right)^2 + g^2 \right) \right), \quad (7.47)$$

where $\hat{f}(\eta; p)$, $\hat{g}(\eta; p)$ and $\hat{\theta}(\eta; p)$ are unknown functions with respect to η and p . \hbar_f , \hbar_g and \hbar_θ are the non-zero auxiliary parameters and N_f , N_g and N_θ are the nonlinear operators.

Also, $p \in (0, 1)$ is an embedding parameter. For $p = 0$ and $p = 1$,

$$\hat{f}(\eta; 0) = f_0(\eta), \hat{f}(\eta; 1) = f(\eta), \quad (7.48)$$

$$\hat{g}(\eta; 0) = g_0(\eta), \hat{g}(\eta; 1) = g(\eta), \quad (7.49)$$

$$\hat{\theta}(\eta; 0) = \theta_0(\eta), \hat{\theta}(\eta; 1) = \theta(\eta). \quad (7.50)$$

In other words, when variation of p is taken from 0 to 1 then $\hat{f}(\eta; p)$, $\hat{g}(\eta; p)$ and $\hat{\theta}(\eta; p)$ vary from $f_0(\eta)$, $g_0(\eta)$ and $\theta_0(\eta)$ to $f(\eta)$, $g(\eta)$ and $\theta(\eta)$ respectively. Taylor's series expansion of these functions yield the following:

$$\hat{f}(\eta; p) = f_0(\eta) + \sum_{m=1}^{\infty} f_m(\eta)p^m, \quad (7.51)$$

$$\hat{g}(\eta; p) = g_0(\eta) + \sum_{m=1}^{\infty} g_m(\eta)p^m, \quad (7.52)$$

$$\hat{\theta}(\eta; p) = \theta_0(\eta) + \sum_{m=1}^{\infty} \theta_m(\eta)p^m, \quad (7.53)$$

where

$$f_m(\eta) = \frac{1}{m!} \left[\frac{\partial^m f(\eta; p)}{\partial p^m} \right]_{p=0}, \quad (7.54)$$

$$g_m(\eta) = \frac{1}{m!} \left[\frac{\partial^m g(\eta; p)}{\partial p^m} \right]_{p=0}, \quad (7.55)$$

$$\theta_m(\eta) = \frac{1}{m!} \left[\frac{\partial^m \theta(\eta; p)}{\partial p^m} \right]_{p=0}. \quad (7.56)$$

It should be noted that the convergence in the above series strongly depends upon \hbar_f, \hbar_g and \hbar_θ . Assuming that these nonzero auxiliary parameters are chosen so that Equations (7.51) – (7.53) converges at $p = 1$. Hence, one can obtain the following:

$$f(\eta) = f_0(\eta) + \sum_{m=1}^{\infty} f_m(\eta), \quad (7.57)$$

$$g(\eta) = g_0(\eta) + \sum_{m=1}^{\infty} g_m(\eta), \quad (7.58)$$

$$\theta(\eta) = \theta_0(\eta) + \sum_{m=1}^{\infty} \theta_m(\eta). \quad (7.59)$$

Differentiating the zeroth order deformation (7.38) – (7.40) and (7.41) – (7.44) m times with respect to p and substituting $p = 0$, and finally dividing by $m!$, the m^{th} order deformation

($m \geq 1$) is

$$L_f[f_m(\eta) - \chi_m f_{m-1}(\eta)] = \hbar_f R_{f,m}(\eta), \quad (7.60)$$

$$L_g[g_m(\eta) - \chi_m g_{m-1}(\eta)] = \hbar_g R_{g,m}(\eta), \quad (7.61)$$

$$L_\theta[\theta_m(\eta) - \chi_m \theta_{m-1}(\eta)] = \hbar_\theta R_{\theta,m}(\eta), \quad (7.62)$$

subject to the boundary conditions

$$f_m(0) = f'_m(0) = 0, \quad (7.63)$$

$$f_m(1) = f'_m(1) = 0, \quad (7.64)$$

$$g_m(0) = g_m(1) = 0, \quad (7.65)$$

$$\theta_m(0) = \theta_m(1) = 0, \quad (7.66)$$

with

$$R_{f,m}(\eta) = a_1 f_{m-1}^{iv} - Re(\sum_{j=0}^{m-1} f_j' f_{m-1-j}'' - \sum_{j=0}^{m-1} f_j f_{m-1-j}''') - 2Kr g_{m-1}' - \left(a_3 M^2 + \frac{a_1}{k}\right) f_{m-1}'', \quad (7.67)$$

$$R_{g,m}(\eta) = a_1 g_{m-1}'' - Re(\sum_{j=0}^{m-1} f_j' g_{m-1-j} - \sum_{j=0}^{m-1} f_j g_{m-1-j}') + 2Krf_{m-1}' - \left(a_3 M^2 + \frac{a_1}{k}\right) g_{m-1}, \quad (7.68)$$

$$R_{\theta,m}(\eta) = \theta_{m-1}'' + Pr \left(Re a_2 \sum_{j=0}^{m-1} f_j \theta_{m-1-j}' + Eca_4 \left(4 \sum_{j=0}^{m-1} f_j' f_{m-1-j}' + \sum_{j=0}^{m-1} g_j g_{m-1-j} \right) \right), \quad (7.69)$$

With

$$\chi_m = \begin{cases} 0, & m \leq 1 \\ 1, & m > 1 \end{cases}. \quad (7.70)$$

Solving the corresponding m^{th} order deformation equations,

$$f_m(\eta) = f_m^*(\eta) + C_1 + C_2 \eta + C_3 e^\eta + C_4 e^{-\eta}, \quad (7.71)$$

$$g_m(\eta) = g_m^*(\eta) + C_5 + C_6 e^\eta, \tag{7.72}$$

$$\theta_m(\eta) = \theta_m^*(\eta) + C_7 + C_8 \eta. \tag{7.73}$$

Here f_m^* , g_m^* and θ_m^* are given by are particular solution of the corresponding m^{th} order equations and the constants C_i ($i = 1, 2, \dots, 8$) are to be determined by the boundary conditions.

7.4.1 Convergence of solutions

Convergence of the HAM solutions and their rate of approximations strongly depend on the values of the auxiliary parameters \hbar_f , \hbar_g and \hbar_θ . For this purpose the associated h-curves are plotted in Figure 7.2. It clearly suggests admissible range for the auxiliary parameters.

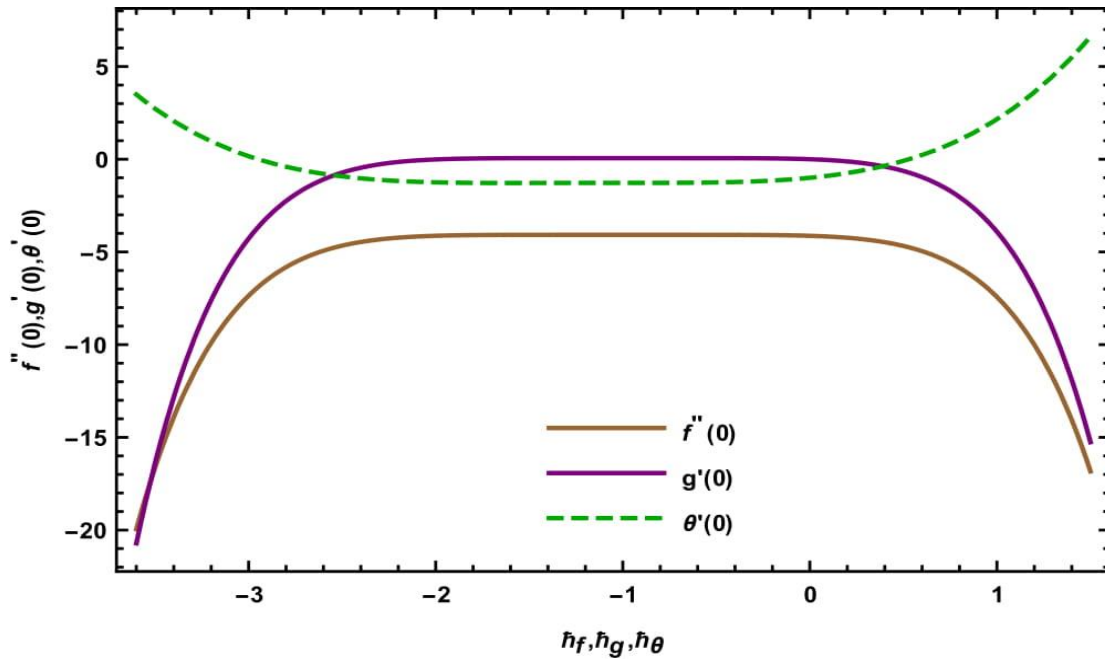


Figure 7.2: H-Curve of $f''(0), g'(0), \theta'(0)$ for different values of $\hbar_f, \hbar_g, \hbar_\theta$ at $M = 1$, $Kr = 1, Pr = 7.2, Ec = 0.01, \phi = 0.04, \kappa = 0.2, Nr = 0.1$ and $Re = 0.1$.

7.5 Results and Discussion

In this section, to acquire a rich understanding on the physics of the problem, the solutions are obtained using appropriate codes in Mathematica. Obtained results are explained with the help of graphs. Parametric study is performed for Reynolds number Re , Radiation parameter Nr ,

Magnetic parameter M , nanoparticle volume fraction ϕ , Permeability parameter κ and Rotation parameter Kr in Figures 7.3 – 7.18.

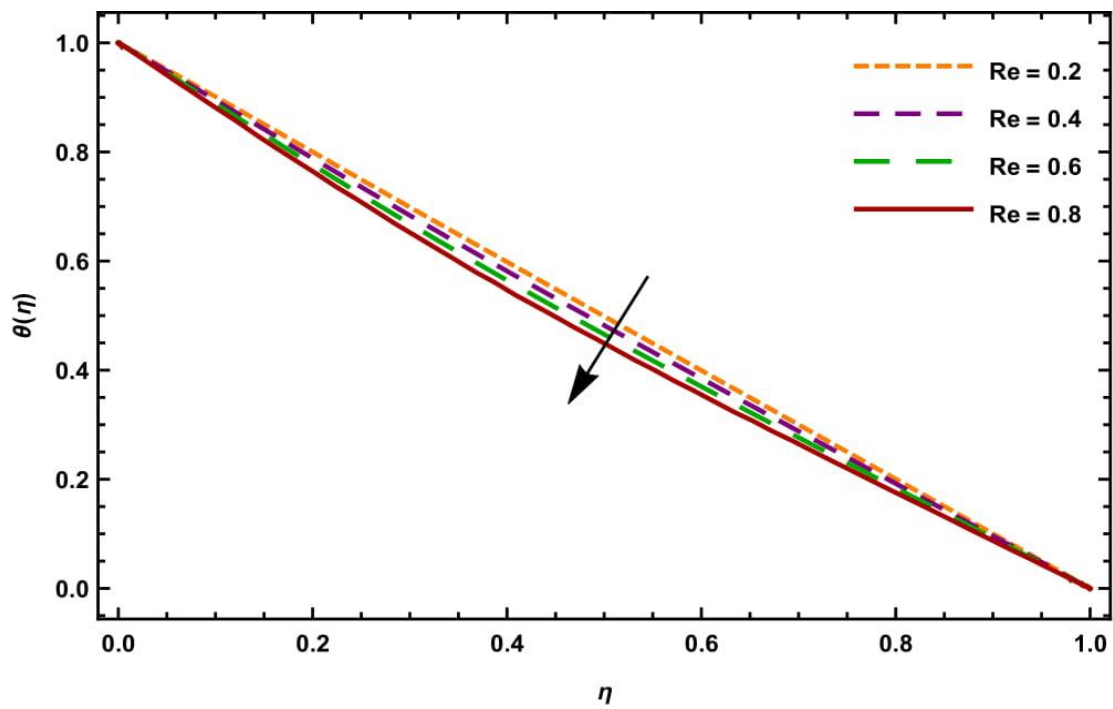


Figure 7.3: Temperature Profile θ for different values of η and Re at $M = 1, Kr = 1, Pr = 7.2, Ec = 0.01, \phi = 0.04, \kappa = 0.2$ and $Nr = 0.1$.

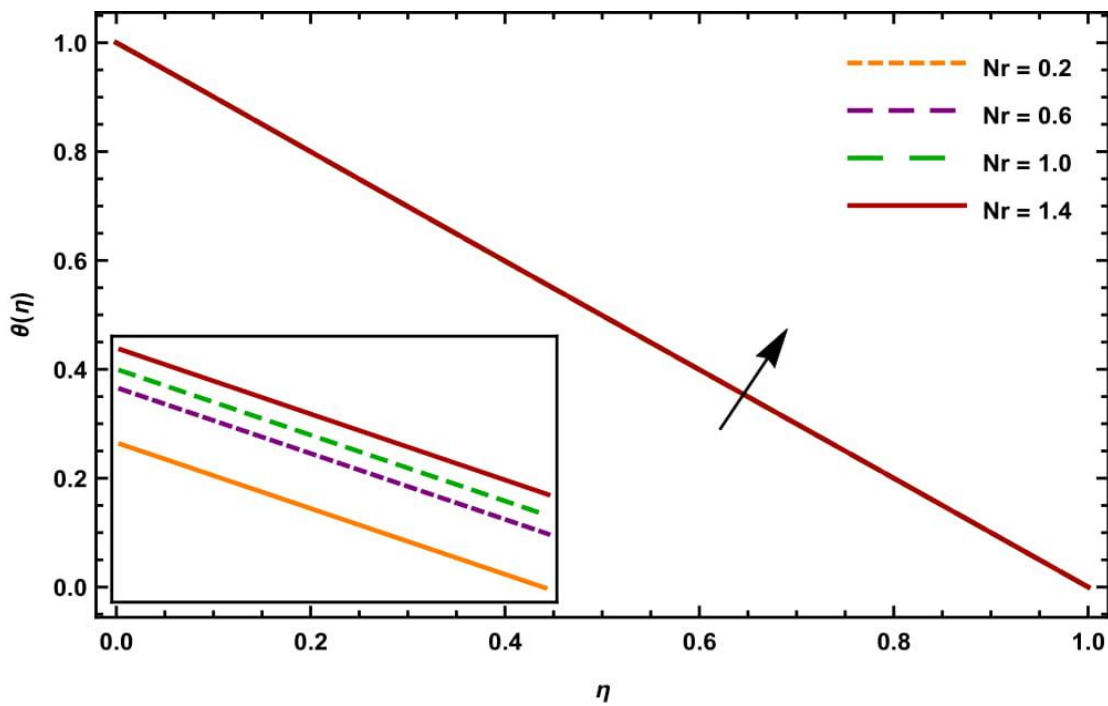


Figure 7.4: Temperature Profile θ for different values of η and Nr at $M = 1, Kr = 1, Pr = 7.2, Ec = 0.01, \phi = 0.04, \kappa = 0.2$ and $Re = 0.1$.

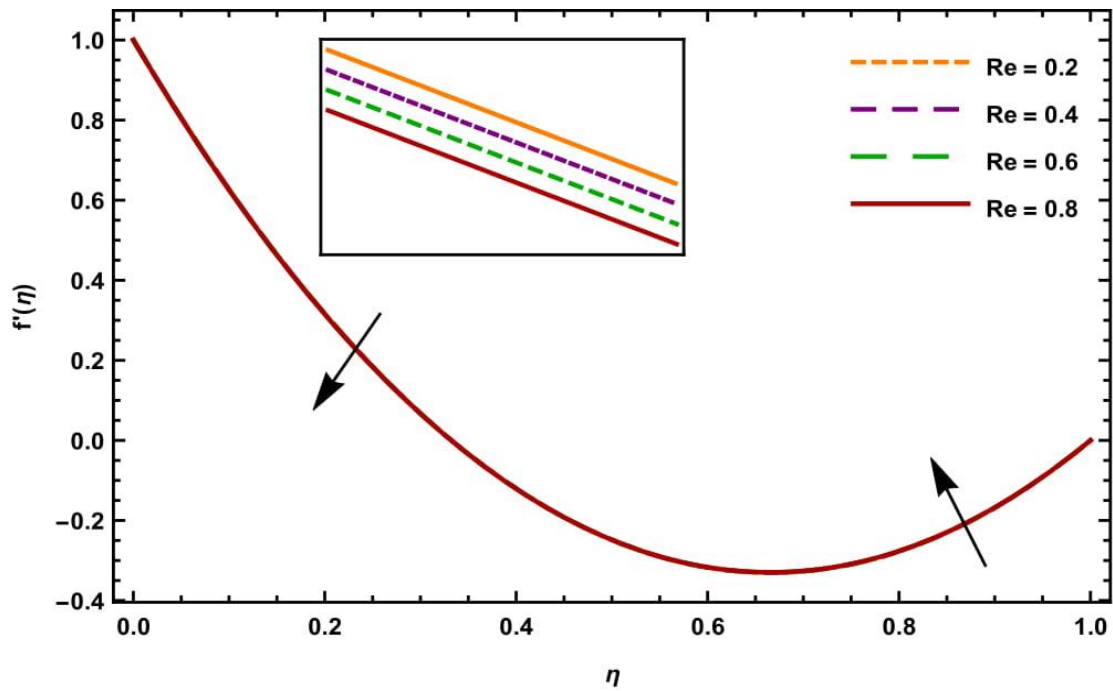


Figure 7.5: Velocity profile f' for different values of η and Re at $M = 1, Kr = 1, Pr = 7.2, Ec = 0.01, \phi = 0.04, \kappa = 0.2$ and $Nr = 0.1$.

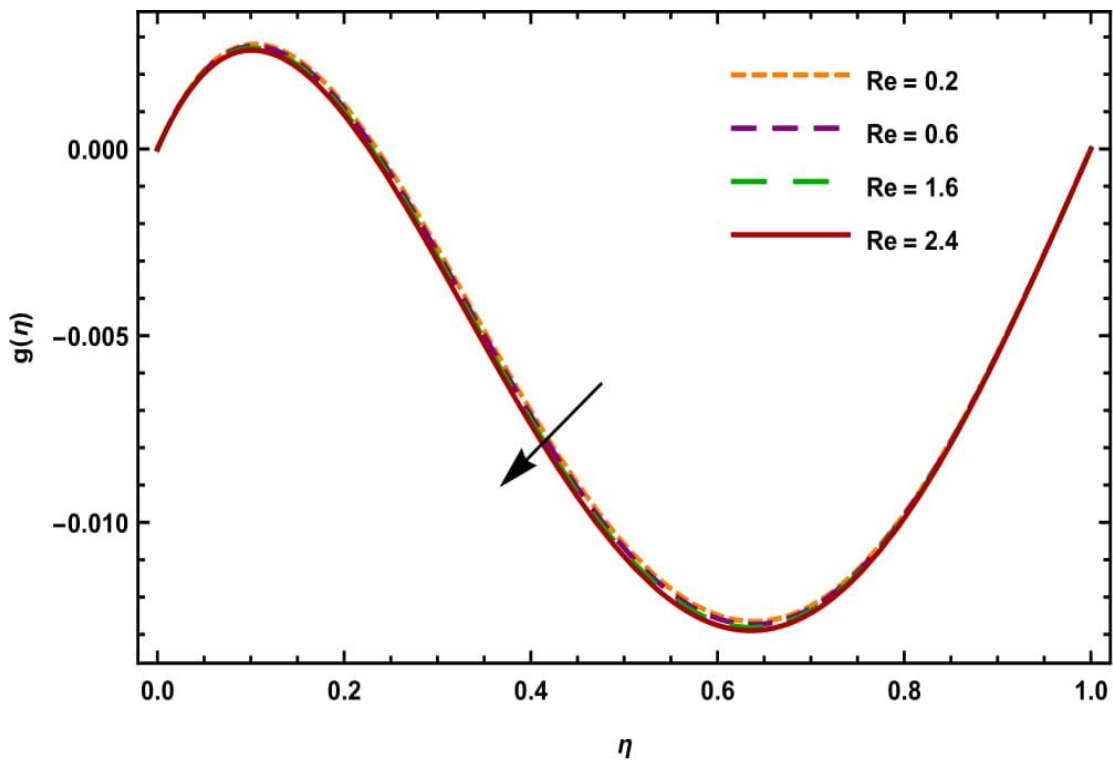


Figure 7.6: Velocity profile g for different values of η and Re at $M = 1, Kr = 1, Pr = 7.2, Ec = 0.01, \phi = 0.04, \kappa = 0.2$ and $Nr = 0.1$.

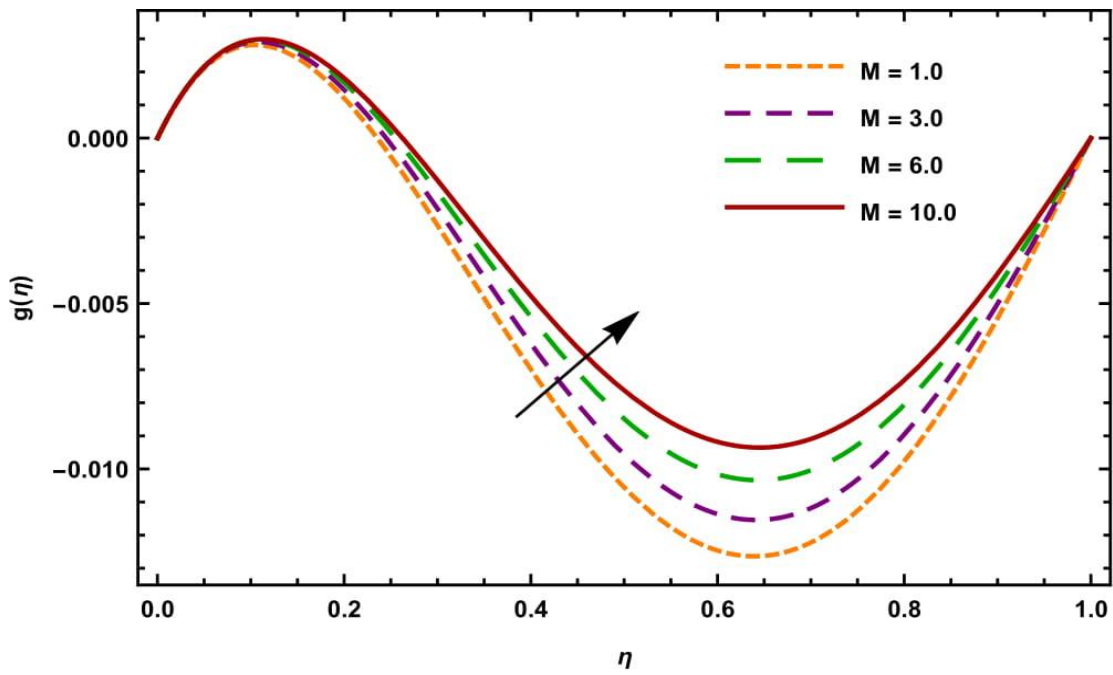


Figure 7.7: Velocity profile g for different values of η and M at $Re = 0.1, Kr = 1$, $Pr = 7.2, Ec = 0.01, \phi = 0.04, \kappa = 0.2$ and $Nr = 0.1$.

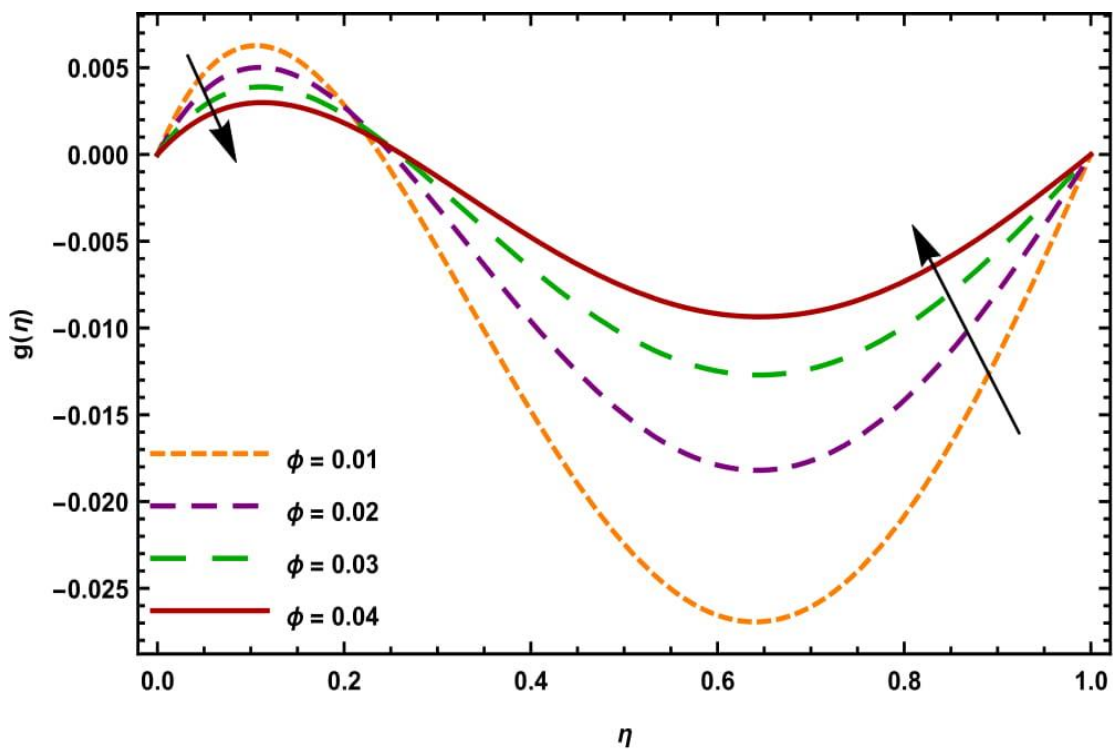


Figure 7.8: Velocity profile g for different values of η and ϕ at $Re = 0.1, Kr = 1$, $Pr = 7.2, Ec = 0.01, M = 1, \kappa = 0.2$ and $Nr = 0.1$.

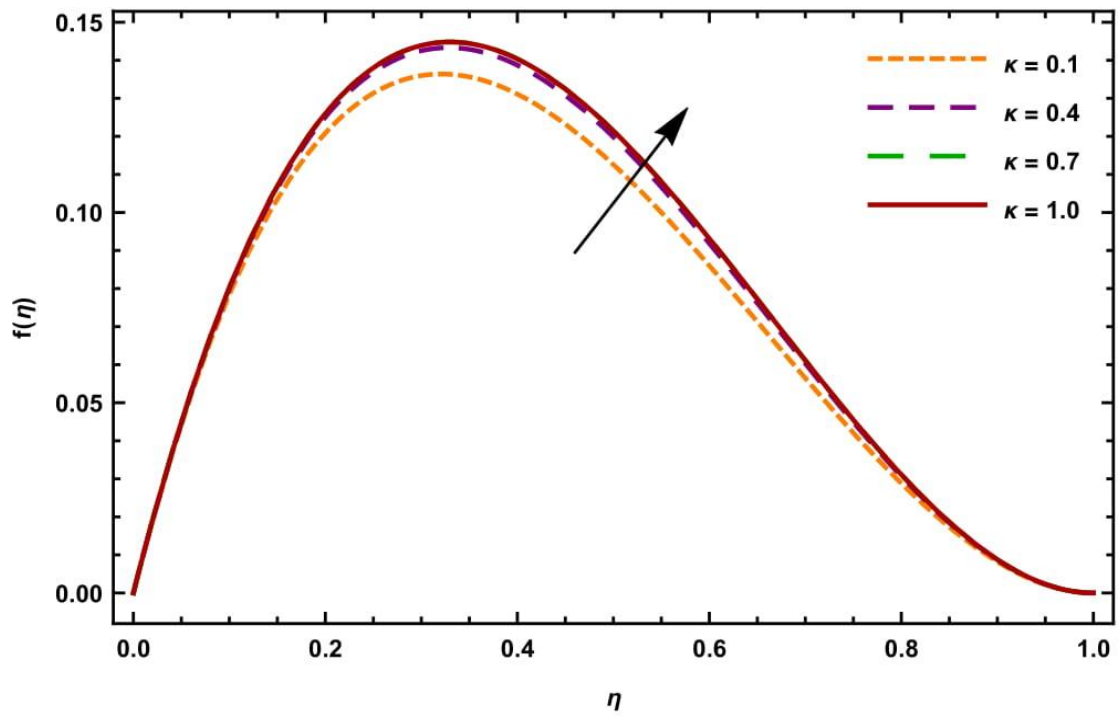


Figure 7.9: Velocity profile f for different values of η and κ at $Re = 0.1, Kr = 1, Pr = 7.2, Ec = 0.01, M = 1, \phi = 0.04$ and $Nr = 0.1$.

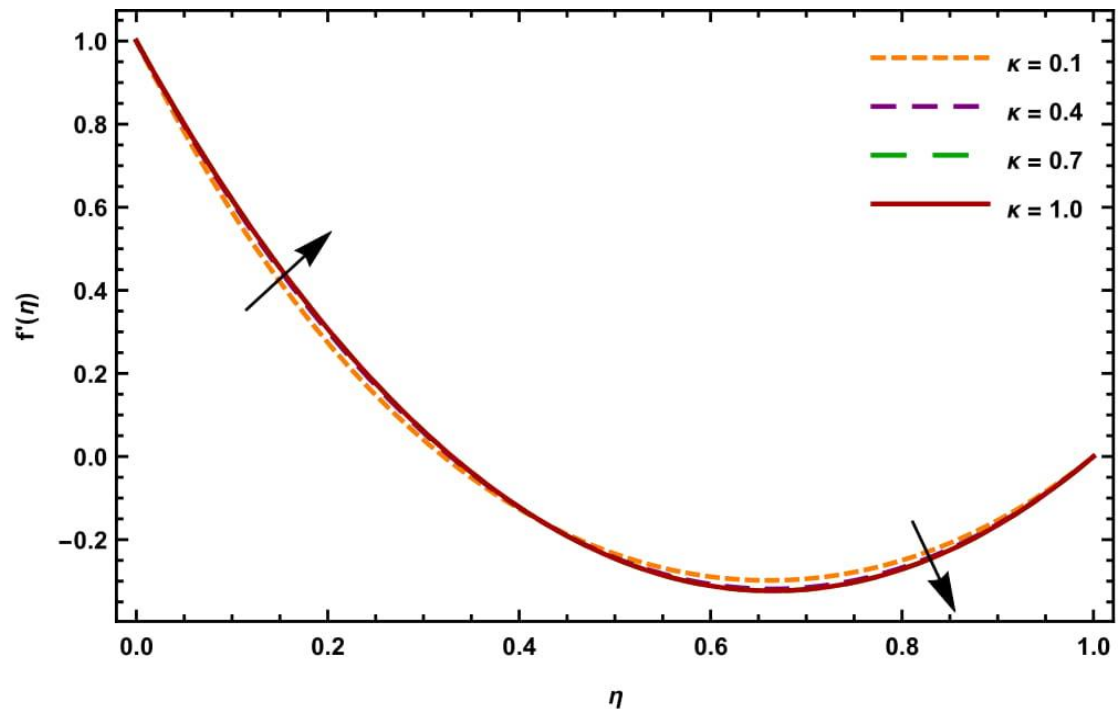


Figure 7.10: Velocity profile f' for different values of η and κ at $Re = 0.1, Kr = 1, Pr = 7.2, Ec = 0.01, M = 1, \phi = 0.04$ and $Nr = 0.1$.

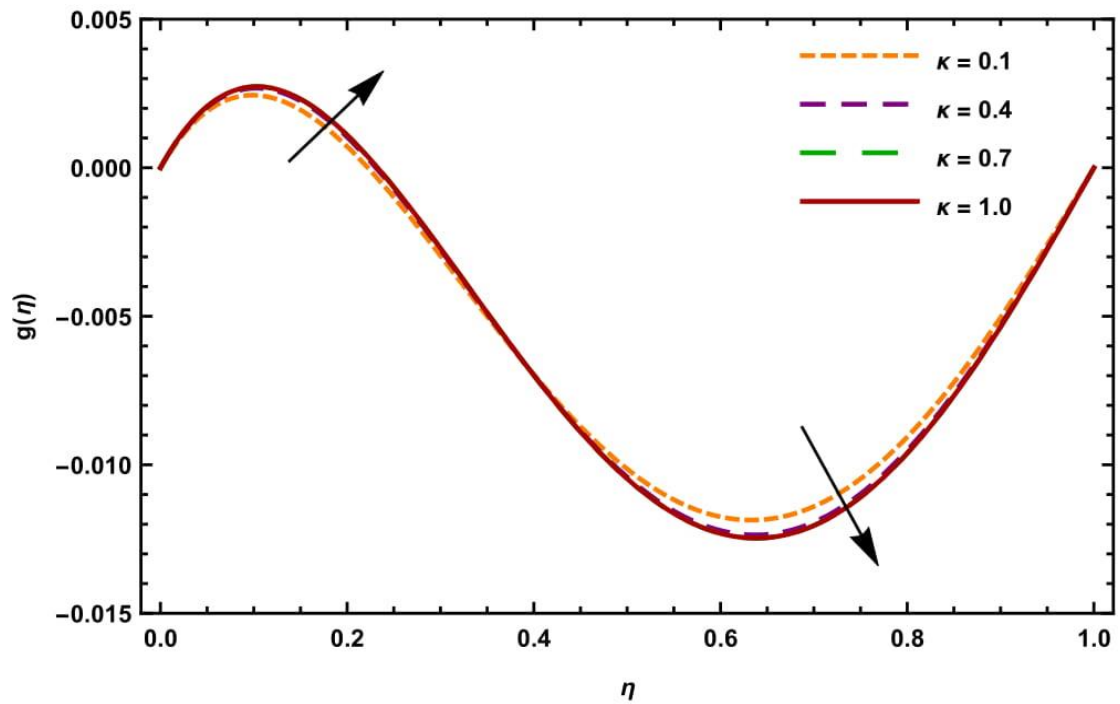


Figure 7.11: Velocity profile g for different values of η and κ at $Re = 0.1, Kr = 1$, $Pr = 7.2, Ec = 0.01, M = 1, \phi = 0.04$ and $Nr = 0.1$.

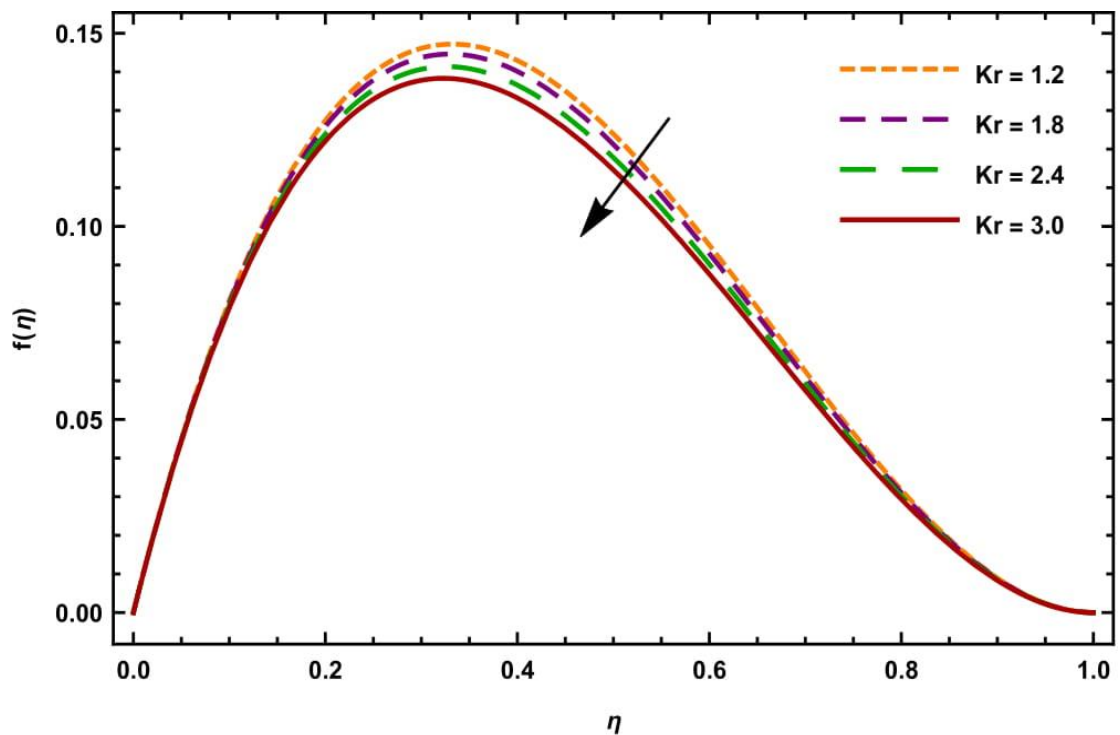


Figure 7.12: Velocity profile f for different values of η and Kr at $Re = 0.1, \kappa = 0.2$, $Pr = 7.2, Ec = 0.01, M = 1, \phi = 0.04$ and $Nr = 0.1$.

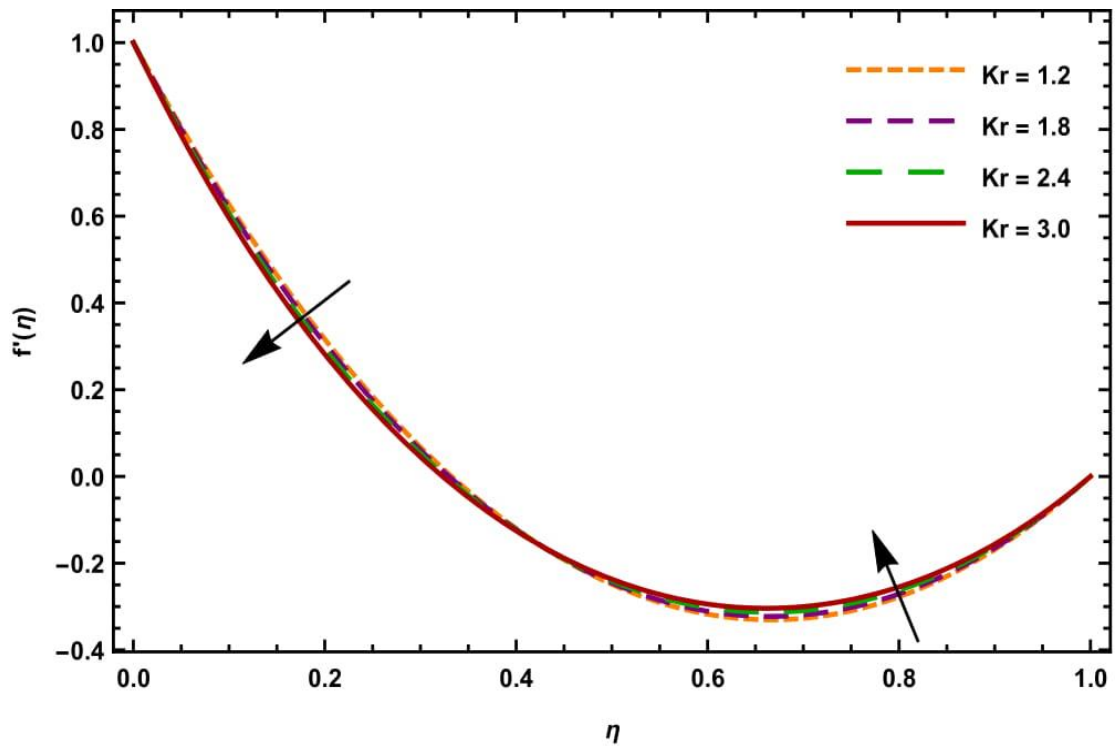


Figure 7.13: Velocity profile f' for different values of η and Kr at $Re = 0.1$, $\kappa = 0.2$, $Pr = 7.2$, $Ec = 0.01$, $M = 1$, $\phi = 0.04$ and $Nr = 0.1$.

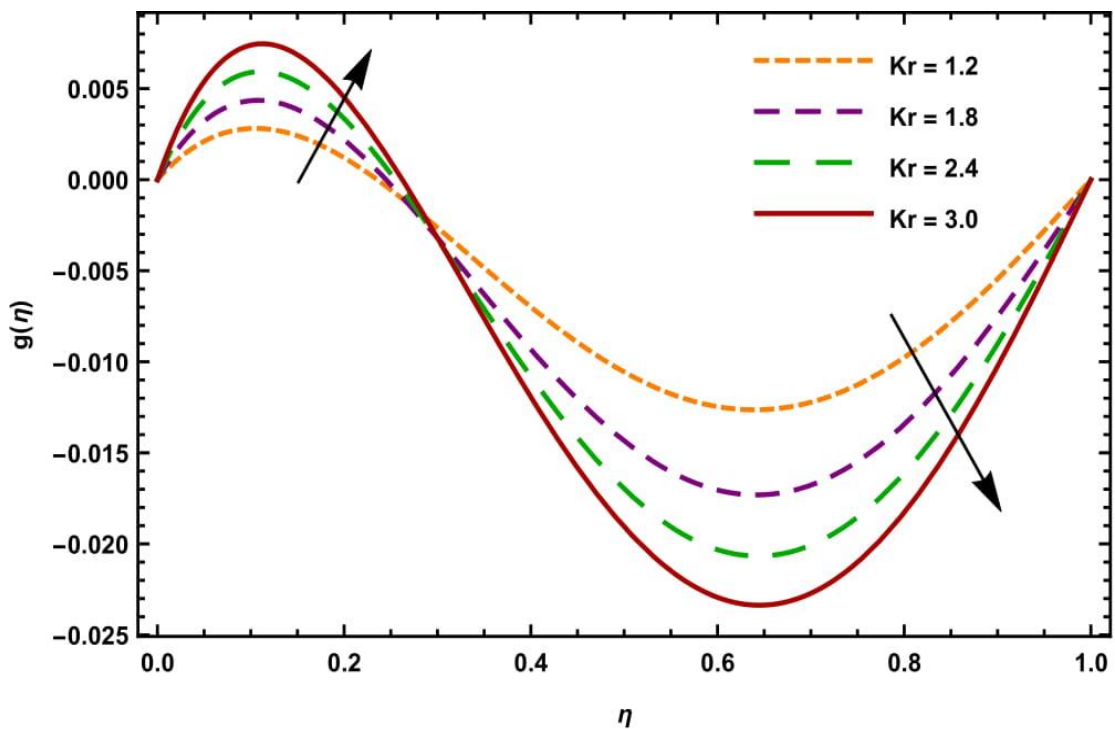


Figure 7.14: Velocity profile g for different values of η and Kr at $Re = 0.1$, $\kappa = 0.2$, $Pr = 7.2$, $Ec = 0.01$, $M = 1$, $\phi = 0.04$ and $Nr = 0.1$.

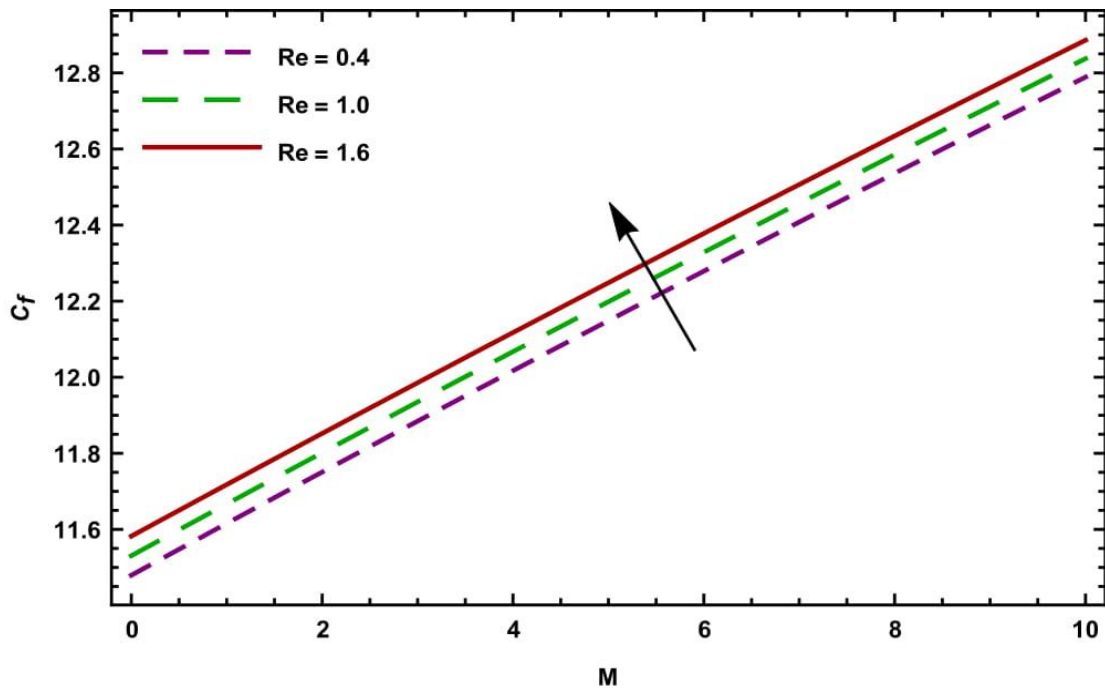


Figure 7.15: Effect of magnetic parameter M and Re on Skin friction coefficient at $Kr = 1, \kappa = 0.2, Pr = 7.2, Ec = 0.01, M = 1, \phi = 0.04$ and $Nr = 0.1$.

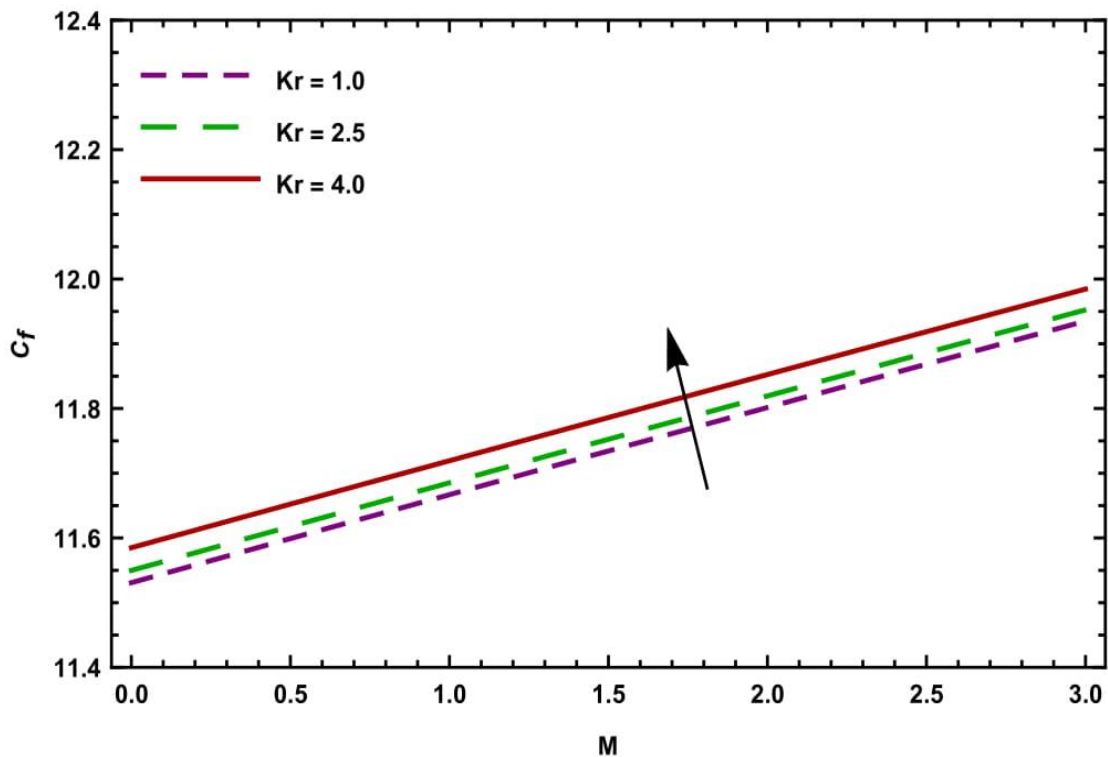


Figure 7.16: Effect of magnetic parameter M and Kr on Skin friction coefficient at $\phi = 0.04, \kappa = 0.2, Pr = 7.2, Ec = 0.01, M = 1, Re = 0.1$ and $Nr = 0.1$.

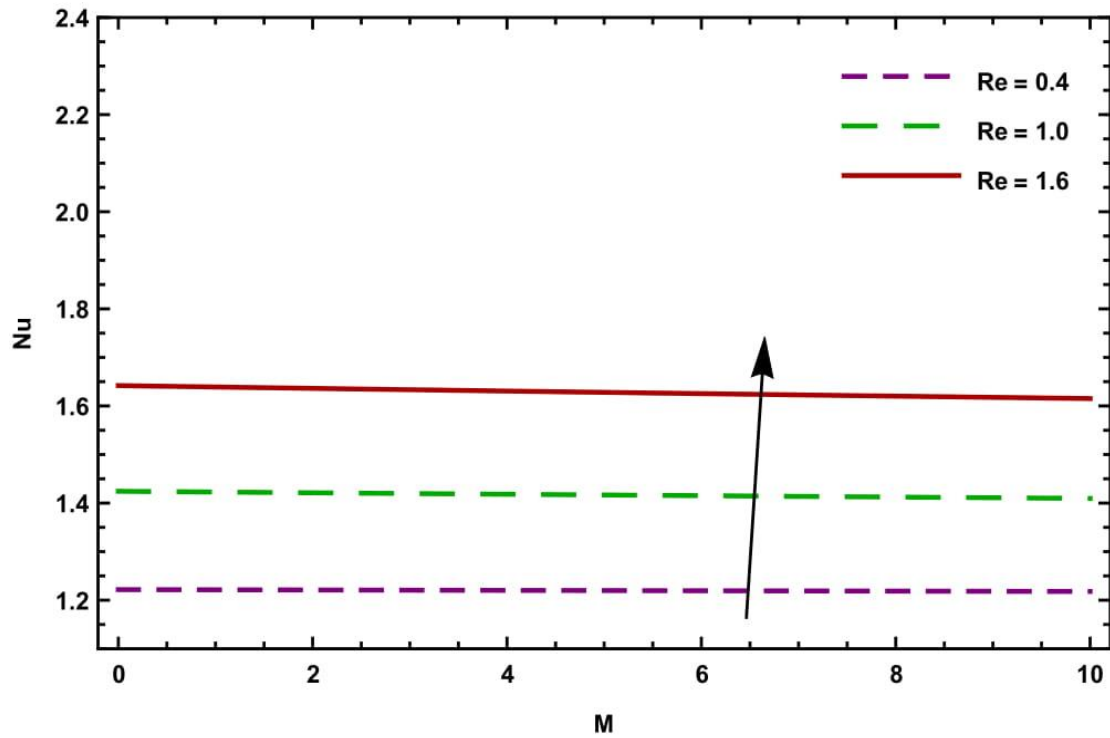


Figure 7.17: Effect of magnetic parameter M and Re on Nusselt number at $\phi = 0.04$, $\kappa = 0.2$, $Pr = 7.2$, $Ec = 0.01$, $M = 1$, $Kr = 1$ and $Nr = 0.1$.

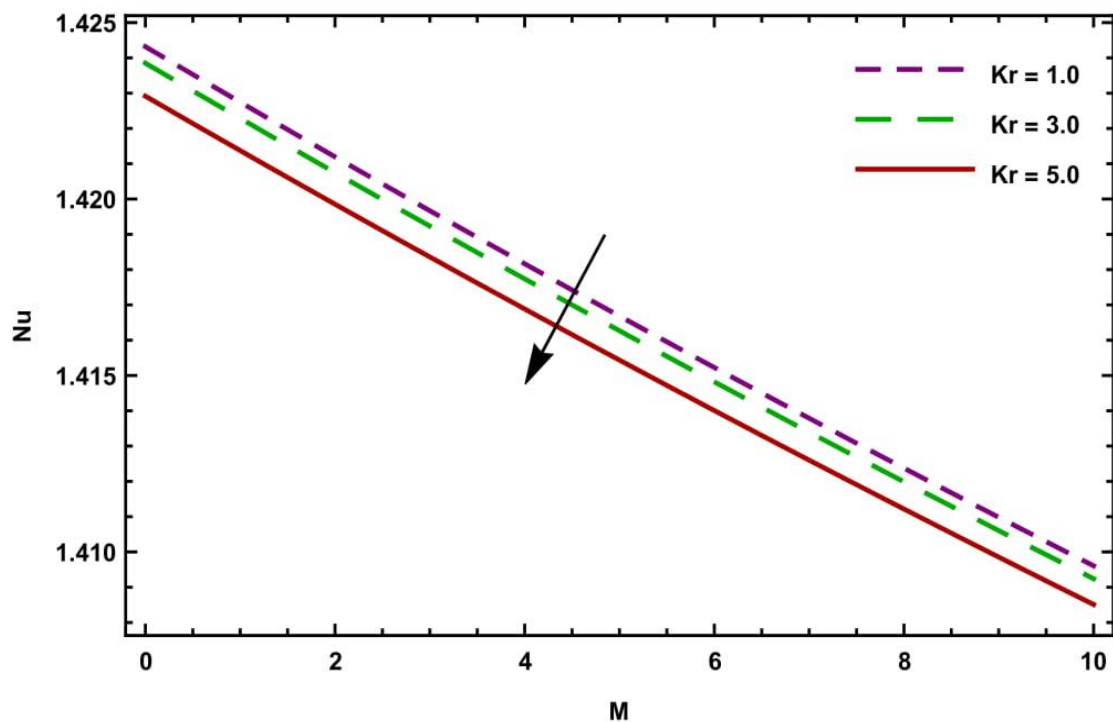


Figure 7.18: Effect of magnetic parameter M and Kr on Nusselt number at $Re = 0.1$, $\kappa = 0.2$, $Pr = 7.2$, $Ec = 0.01$, $M = 1$, $\phi = 0.04$ and $Nr = 0.1$.

Figure 7.3 demonstrates the effects of Reynolds number on temperature profile. It is observed that temperature boundary layer thicknesses diminishes with an intensification of Reynolds number. Figure 7.4 illustrates that temperature increases with radiation. Figures 7.5 – 7.14 show effects of different parameters on velocity profile. Figure 7.5 and 7.6 depict that velocity decreases with rise in Reynolds number Re . It is justified as Reynolds number signifies the inertia effect over the viscous effect. It is evident from Figure 7.7 that velocity component in z direction increases with magnetic field. Figure 7.8 illustrates role of nanoparticle volume fraction on fluid flow. Figures 7.9 – 7.11 show effects of permeability parameter κ on velocity profile. It is observed that velocity increases with increase in κ . Physically it is justified as the resistance of the medium decreases which increase in values of κ . Decrease in f and f' whereas increase in g with increasing values of rotation parameter Kr are observed through Figures 7.12 – 7.14. Effect of Reynolds number on skin friction can be found in Figure 7.15. It is clear that Skin friction increases with increase in Re . Figure 7.16 shows that skin friction can also be decayed by decreasing rotation parameter Kr . Effects of pertinent parameters like Reynolds number Re and rotation parameter Kr on Nusselt number are shown in Figures 7.17 and 7.18 respectively. It is observed that the Nusselt number has a direct stimulus with Reynolds number Re but, it has a conflicting association with the rotation parameter Kr .

7.6 Conclusion

The most important concluding remarks can be summarized as follows:

- Nanofluid velocity declines with escalation in Reynolds number Re and Nanoparticle volume fraction parameter ϕ .
- Nanofluid velocity increases with permeability parameter κ .
- Nanofluid temperature can be increased by increasing of radiation parameter Nr .
- Nanofluid temperature tends to decrease with rising values of Reynolds number Re .

- Skin friction can be reduced by decreasing Reynolds number Re or the rotation parameter Kr .
- Nusselt number decreases with increase in the rotation parameter Kr .